Langmuir
Article
pubs.acs.org/Langmuir

An X-ray Spectromicroscopy Study of Protein Adsorption to Polystyrene−Poly(ethylene oxide) Blends

Bonnie O. Leung,[†] Adam P. Hitchcock,*[,†] John L. Brash,[‡] Andreas Scholl,[§] and Andrew Doran[§]

[†]*Department of Chemistry & Chemical Biology, McMaster University, Hamilton, ON, Canada L8S 4M1,*
[‡]*School of Biomedical Engineering, McMaster University, Hamilton, ON, Canada L8S 4M1, and*
[§]*Advanced Light Source, Lawrence Berkeley National Laboratory, Berkeley, California 94720*

Received June 15, 2010. Revised Manuscript Received July 30, 2010

Synchrotron-based X-ray photoemission electron microscopy (X-PEEM) and atomic force microscopy (AFM) were used to characterize the composition and surface morphology of thin films of a polystyrene−poly(ethylene oxide) blend (PS−PEO), spun cast from dichloromethane at various mass ratios and polymer concentrations. X-PEEM reveals incomplete segregation with ∼30% of PS in the PEO region and vice versa. Protein (human serum albumin) adsorption studies show that this partial phase separation leads to greater protein repellency in the PS region, whereas more protein is detected in the PEO region compared to control samples.

1. Introduction

Biofouling, or the uncontrolled accumulation and persistent adhesion of biological material to surfaces, occurs when the surface fails to replicate the natural structure and function at the contact site.[1,2] The initial step in this biological cascade begins with rapid adsorption of proteins to the material surface.[3] Thus, investigations of protein selectivity in the first steps of protein adsorption to candidate biomaterials can give insights into mechanisms of biocompatibility.

Poly(ethylene oxide) (PEO) and poly(ethylene glycol) (PEG) based composites are important blood compatible materials.[4,5] Self-assembled monolayers (SAMs) of PEO[6] and also PEO-grafted polymers[7] have been documented to show low bioadhesion, with the short, highly dense PEO chains ("brush") preventing the protein from "seeing" the underlying substrate.[8] High molecular weight PEO is also effective in preventing protein adsorption, with the polymer strands at the surface forming loops and tails extending into the aqueous medium.[9] PEO has been blended with a variety of synthetic and natural materials such as polylactide,[10] collagen,[11] *Bombyx mori* silk,[12] and many others to form fibers, scaffolds, and drug carriers with improved biocompatibility and stealth capabilities. Grainger et al.[13] also saw that the incorporation of PEO to PS resulted in decreased protein adsorption. Their study varied the amount of the hydrophilic component in their PS−PEO block copolymer films and found decreased human serum albumin (HSA) adsorption with increasing hydrophilic ratios.

PEO is a water-soluble polymer and mass loss occurs upon exposure of PEO and PEO-rich surfaces to aqueous solutions. Several techniques to cross-link PEO have been successful, including γ,[14] UV,[15,16] and electron irradiation.[17] In particular, UV-initiated cross-linking of PEO with pentaerythritol triacrylate (PETA) was shown to occur even in the solid state.[18] Fluorescence microscopy obtained via integral geometry analysis showed that a PEO surface cross-linked with PETA resulted in a vestigial amount of adsorbed lectin compared to poly(methyl methacrylate) (PMMA) or polystyrene (PS) surfaces.[19]

Although many claims of PEO-based nonfouling surfaces are available in patents and the literature, Kingshott and Griesser[1] caution that detailed and reliable characterization of candidate biomaterial surfaces must be completed to exclude problems such as contamination and surface defects, followed by a sufficiently sensitive technique to measure amounts and locations of protein adsorption. X-ray spectromicroscopy based on surface sensitive X-ray photoemission electron microscopy (X-PEEM) has been shown to be an effective spatially resolved technique for near-surface characterization, and also quantification of biomolecules adsorbed to the near-surface of model biomaterials, with the advantage that it can simultaneously probe the adsorbed biomolecules and the near-surface region of the substrate since its sampling depth (∼10 nm) encompasses both regions. Previously we have used X-PEEM to study materials such as PS−polylactide (PS−PLA)[20] and PS−PMMA[21] and to make systematic studies of the adsorption of human serum albumin (HSA) or fibrinogen

*Corresponding author. E-mail: aph@mcmaster.ca.

(1) Kingshott, P.; Griesser, H. J. *Curr. Opin. Solid State Mater. Sci.* **1999**, *4*, 403–412.
(2) Wedler, F. C.; Riedhammer, T. M. *Biocompat. Clin. Pract.* **1982**, *11*, 1–12.
(3) Castner, D. G.; Ratner, B. D. Biomedical surface science: Foundations to frontiers. *Surf. Sci.* **2002**, *500*, 28–60.
(4) Park, J. H.; Park, K. D.; Bae, Y. H. *Biomaterials* **1999**, *20*, 943.
(5) Bergstrom, K.; Holmberg, K.; Safranj, A.; Hoffman, A. S. *J. Biomed. Mater. Res.* **1992**, *26*, 779.
(6) Prime, K. L.; Whitesides, G. M. *Science* **1991**, *252*, 1164–1167.
(7) Park, J. Y.; Acar, M. H.; Akthakul, A.; Kuhlman, W.; Mayes, A. M. *Biomaterials* **2006**, *27*, 856–865.
(8) Jeon, S. I.; Lee, J. H.; Andrade, J. D.; De Gennes, P. G. *J. Colloid Interface Sci.* **1991**, *142*, 149–158.
(9) Lee, J. H.; Lee, H. B.; Andrade, J. D. *Prog. Polym. Sci.* **1995**, *20*, 1043–1079.
(10) Ahmed, F.; Discher, D. E. *J. Controlled Release* **2004**, *96*, 37–53.
(11) Matthews, J. A.; Simpson, D. G.; Wnek, G. E.; Bowlin, G. L. *Biomacromolecules* **2002**, *3*, 232–238.
(12) Jin, H. J.; Fridrikh, S. V.; Rutledge, G. C.; Kaplan, D. L. *Biomacromolecules* **2002**, *3*, 1233–1239.
(13) Grainger, D., Okano, T., Kim, S. W. *Advances in Biomedical Polymers*; Gebelein, C. G., Ed.; Plenum Publishing Corporation: New York, 1987.
(14) Stringer, J. L.; Peppas, N. A. *J. Controlled Release* **1996**, *42*, 195–202.
(15) Doycheva, M.; Petrova, E.; Stamenova, R.; Tsvetanov, C.; Riess, G. *Macrmol. Mater. Eng.* **2004**, *289*, 676–680.
(16) Mellott, M. B.; Searcy, K.; Pishko, M. V. *Biomaterials* **2001**, *22*, 929–941.
(17) Kofinas, P.; Athanassiou, V.; Merrill, E. W. *Biomaterials* **1996**, *17*, 1547–1550.
(18) Doytcheva, M.; Dotcheva, D.; Stamenova, R.; Tsvetanov, C. *Macrmol. Mater. Eng.* **2001**, *286*, 30–33.
(19) Zemla, J.; Lekka, M.; Wiltowska-Zuber, J.; Budkowski, A.; Rysz, J.; Raczkowska, J. *Langmuir* **2008**, *24*, 10253–10258.

(Fg) to these surfaces as a function of protein concentration,[22] exposure time,[22] pH,[23] ionic strength,[24] protein-peptide competitive adsorption[25] and polymer surface rugosity.[24] This work has demonstrated that protein adsorption is controlled mainly by hydrophobic effects. Furthermore, our systematic study probing the effect of PETA cross-linker on the biocompatibility of PEO revealed that a detectable amount of HSA adsorbs to the cross-linked surface when the concentration of PETA exceeds 5 wt %.[26]

Here we report the chemical composition and surface morphology of PS−PEO thin films spun cast from various mass ratios and polymer concentrations, followed by evaluation of these surfaces as candidate biomaterials. Previously, films created from diblock copolymers of PS−PEO, which formed PEO nanocylinders in a matrix of PS, were shown to significantly reduce the adsorption of bovine serum albumin (BSA), lysozyme, and fibrinogen (Fg) compared to control PS surfaces.[27] Protein adsorption was characterized by quartz crystal microbalance with dissipation (QCM-D), and atomic force microscopy (AFM). In our study, we spatially map the distribution of HSA across the surface of the PS−PEO blends, and quantify the amount of HSA adsorbed to the PS, PEO, and interface regions.

This present study is part of an ongoing effort to provide insight into the interaction of blood and blood components with phase-segregated and patterned model biomaterials. These results are intended to contribute toward further understanding of the fundamentals of protein adsorption, which may lead to the development of improved blood- and tissue-contacting medical devices.

2. Materials and Methods

2.1. Materials. Polystyrene (MW = 1.07 M) and poly(ethylene oxide) (MW = 600 K) were obtained from Polymer Source Inc. and Sigma-Aldrich, respectively, and PETA was purchased from Sigma-Aldrich, and used as received. PS−PEO films composed of different mass ratios and concentrations were spun cast (4000 rpm, 40 s) from dichloromethane onto a clean 1 × 1 cm native oxide silicon wafer (Wafer World, Inc.) and degreased with trichloroethylene, acetone, and methanol, followed by rinsing with doubly deionized water (DDI).

Human serum albumin (HSA) was purchased from Behringwerke AG, Marburg, Germany, and found to be homogeneous as judged by sodium dodecyl sulfate polyacrylamide gel electrophoresis (SDS-PAGE). Protein solutions for exposure were prepared from DDI water using HSA concentrations of 0.05, 0.01, or 0.005 mg/mL.

2.2. Substrates and Protein Exposure. PS and PEO were dissolved in dichloromethane (total weight 50 mg, 1 wt %) at predetermined mass ratios. PETA (1 wt % of the total polymer weight) was added before the solution was spun cast onto a clean silicon wafer. After dilution, PS and PEO mass ratios were lowered to 0.5 wt %. To test the effect of annealing, the PS−PEO films were annealed at 160 °C for 18 h in a vacuum oven at a pressure ~10^{-5} Torr, achieved with a cryo-trapped turbo pump. Next, the substrates were cross-linked by exposure to a 365 nm UV lamp under flowing nitrogen for 40 min. The UV reactor consists of five RPR Rayonet photochemical reaction lamps positioned ~5 cm above the samples. No filters or initiators were used. The morphology of these substrates was then characterized by atomic force microscopy (AFM) and X-ray spectromicroscopy.

For protein adsorption studies, unannealed (cross-linked and noncross-linked) films of PS:PEO 60:40 (0.5 wt %) were placed in a beaker, covered with 5 mL of 0.05, 0.01, or 0.005 mg/mL aqueous protein solution for 20 min and then diluted three times with at least 50 mL of doubly deionized water. The substrates were removed and vigorously rinsed. Residual water on the surface of the protein adsorbed sample was then carefully removed by touching the edge of the Si wafer with lens paper.

2.3. Atomic Force Microscopy (AFM). All AFM images were acquired with a Quesant Q-scope 250 (Quesant Instruments, Ambios Technology, Santa Cruz, CA), operated in noncontact mode. Standard noncontact silicon cantilevers from Quesant were used. Phase and height mode images (5 × 5 μm or 15 × 15 μm) were collected simultaneously at a scan rate of 1.8−2.0 Hz under ambient conditions.

AFM was used to verify that the PEO was cross-linked and polymer did not leach into aqueous solution upon exposure to water. A PS−PEO 40:60 film was spun cast from dichloromethane and the same surface was imaged prior and after water exposure (Supporting Information, Figure 1). The surface morphology remained the same, even though the AFM images were taken at different locations, showing that the film surface did not dissolve/leach after exposure to water for 20 min.

2.4. STXM. The polymer scanning transmission X-ray microscope (STXM) on beamline 5.3.2 at the Advanced Light Source (ALS) in Berkeley, CA was used to collect high quality near-edge X-ray absorption fine structure (NEXAFS) reference spectra of PS, PEO and HSA.[28,29] The polymer STXM operates in transmission mode and the experimental beamline setup offers slightly better energy resolution (0.1−0.2 eV) compared to X-PEEM (0.4−0.5 eV); however, similar NEXAFS line shapes are obtained from both methods. Samples were prepared by solvent-casting on an X-ray transparent window with resulting film thickness below 100 nm. To minimize radiation damage, the spectra of micrometer size areas were measured with a defocused beam using image sequences.[30] An image at a damage sensitive energy was recorded after each image sequence measurement to ensure negligible damage. The intensity scale of each reference spectrum was normalized to the signal expected from 1 nm of the polymer or protein at its bulk density.

2.5. X-PEEM. All X-PEEM data were collected at the ALS on bend magnet beamline 7.3.1 with the PEEM-2 microscope. Detailed accounts of the experimental apparatus, beamline setup and instrument optics have been presented previously.[31] In short, primary photoelectrons and secondary electrons are ejected by the absorption of 70−80% right or left circularly polarized monochromatic X-rays and accelerated into an electrostatic imaging column, where the spatial distribution is magnified and detected by a charge coupled device (CCD) camera. X-PEEM is a total electron yield technique with a strong detection for low kinetic energy secondary electrons. X-PEEM is a highly surface sensitive microscope with an attenuation depth (1/e) of 4 nm for

(20) Leung, B. O.; Hitchcock, A. P.; Brash, J. L.; Scholl, A.; Doran, A. *Macromolecules* **2009**, *42*, 1679–1684.
(21) Morin, C.; Hitchcock, A. P.; Cornelius, R. M.; Brash, J. L.; Scholl, A.; Doran, A. *J. Elec. Spectrosc.* **2004**, *137−140*, 785–794.
(22) Li, L.; Hitchcock, A. P.; Robar, N.; Cornelius, R.; Brash, J. L.; Scholl, A.; Doran, A. *J. Phys. Chem B* **2006**, *110*, 16763–16773.
(23) Li, L.; Hitchcock, A. P.; Cornelius, R.; Brash, J. L.; Scholl, A.; Doran, A. *J. Phys. Chem B* **2008**, *112*, 2150–2158.
(24) Leung, B. O.; Hitchcock, A. P.; Cornelius, R. M.; Brash, J. L.; Scholl, A.; Doran, A. *Biomacromolecules* **2009**, *10*, 1838–1845.
(25) Leung, B. O.; Hitchcock, A. P.; Brash, J. L.; Scholl, A.; Doran, A.; Henklein, P.; Overhage, J.; Hilpert, K.; Hale, J. D.; Hancock, R. E. W. *Biointerphases* **2008**, *3*, F27–F35.
(26) Leung, B. O.; Hitchcock, A. P.; Brash, J. L.; Scholl, A.; Doran, A. *Langmuir* **2009**, *25*, 13332–13335.
(27) George, P. A.; Donose, B. C.; Cooper-White, J. J. *Biomaterials* **2009**, *30*, 2449–2456.
(28) Warwick, T.; Ade, H.; Kilcoyne, A. L. D.; Kritscher, M.; Tylisczcak, T.; Fakra, S.; Hitchcock, A. P.; Hitchcock, P.; Padmore, H. A. J. *Synchrotron Radiat.* **2002**, *9*, 254.
(29) Kilcoyne, A. L. D.; Tylisczak, T.; Steele, W. F.; Fakra, S.; Hitchcock, P.; Franck, K.; Anderson, E.; Harteneck, B.; Rightor, E. G.; Mitchell, G. E.; Hitchcock, A. P.; Yang, L.; Warwick, T.; Ade, H. J. *Synchrotron Radiat.* **2003**, *10*, 125.
(30) Jacobsen, C. J.; Zimba, C.; Flynn, G.; Wirick, S. J. *Microscopy* **2000**, *19*, 173–184.
(31) Anders, S.; Padmore, H. A.; Duarte, R. M.; Renner, T.; Stammler, T.; Scholl, A.; Scheinfein, M. R.; Stohr, J.; Seve, L.; Sinkovic, B. *Rev. Sci. Instrum.* **1999**, *70*, 3973.

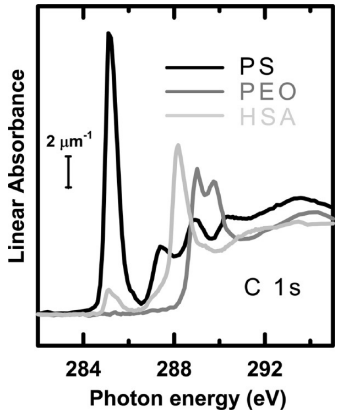

Figure 1. C 1s X-ray absorption spectra of polystyrene (PS, black), poly(ethylene oxide) (PEO, dark gray) and human serum albumin (HSA, light gray), recorded with STXM. The spectra are plotted on an absolute linear absorbance scale.

polymers,[32] with integrated signals probing the top 10 nm of the sample.

A 100 nm thick titanium filter was used to eliminate second-order light. A shutter with a 0.1 s response time was implemented to block the X-ray beam during the time required to transfer images from the CCD camera and during the photon energy step to reduce radiation damage. This resulted in an exposure reduction of 50%. Masking upstream of the monochromator further reduced the incident flux by a factor of ten and a limited number of energies or larger step sizes (23 in C 1s) and a short exposure time (1 s) per image were used as other ways to minimize radiation damage. The field of view was approximately 20 μm.

2.6. X-PEEM Data Analysis. The C 1s reference spectra for PS, PEO and HSA are presented in Figure 1. At the C 1s edge, the spectra can be easily differentiated with PS characterized by its C 1s $\rightarrow \pi^*_{C=C}$ transition at 285.15(3) eV, HSA by its strong C 1s $\rightarrow \pi^*_{C=O}$ transition at 288.20(6) eV, and PEO by C 1s $\rightarrow \sigma^*_{C-H}$ and C 1s $\rightarrow \sigma^*_{C-O}$ transitions at 289.03(8) and 289.78(8) eV, respectively.[33]

The aXis2000 software package[34] was used to analyze the data. C 1s image sequences were aligned if necessary, normalized to the ring current and divided by the I_0 spectrum collected from a clean, HF-etched Si(111) chip. The I_0 spectrum was corrected for the absorption of the underlying silicon and a factor proportional to the photon energy representing the bolometric response of the X-PEEM detection. All carbon stacks were calibrated by assigning the energy of the C 1s $\rightarrow \pi^*_{C=C}$ transition of PS to 285.15 eV.

Singular value decomposition (SVD), an optimized method for least-squares analysis in highly overdetermined data sets,[35,36] was used to fit each pixel of the C 1s image sequence with PS, PEO and HSA reference spectra. The fit coefficients generated from the SVD analysis are presented as component maps which are the spatial distributions of each component. A heavily smoothed image arising from the sum of the component maps was used to correct skewed illumination by dividing each component map with the smoothed image. The intensities were adjusted by dividing the intensity of each image in the image sequence by a scale factor which resulted in a total average thickness (sum of all components) of 10 nm, corresponding to the sampling depth of X-PEEM.[32] We note that while the X-PEEM signal is integrated over the total sampling depth of 10 nm, there is an exponential decay of contributions over this 10 nm range, such that the outermost 1−2 nm at the very surface gives a much larger contribution than the innermost 1−2 nm which is more representative of the bulk.

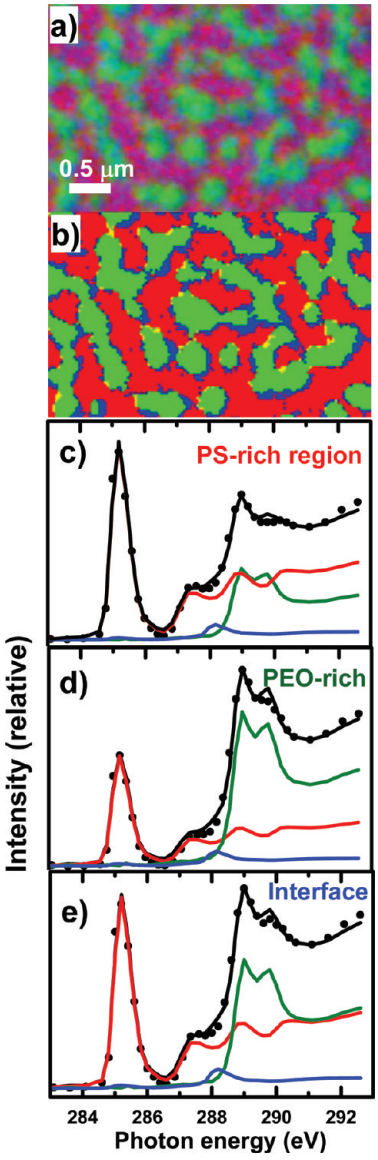

Figure 2. Example of analysis procedures for a C 1s image sequence (23 energies) recorded from a PS/PEO blend thin film spun-cast from a dichloromethane solution with a total loading of 0.5 wt % polymer in a 60:40 PS:PEO ratio with 0.05 mg/mL adsorbed HSA. (a) Color coded composite (nonrescaled) of the PS (red), PEO (green), and HSA (blue) component maps derived from singular value decomposition (SVD) using the pure species reference spectra (Figure 1). (b) Mask used to extract spectra of specific regions. Red denotes PS-rich regions, green denotes PEO-rich regions, defined by threshold masking the PS and PEO component maps. The remaining blue pixels define areas at the interface between the PS-rich and PEO-rich domains. (c) Curve fit of the average C 1s spectrum of the PS-rich region (data, dots; fit, black line; components, colored lines). (d) Curve fit of the average C 1s spectrum of the PEO-rich region (same color coding). (e) Curve fit of the average C 1s spectrum of the interface region (same color coding).

Figure 2 shows an example of the methodology used to extract the quantitative results. After fitting to obtain component maps (presented as a color coded composite in Figure 2a),

(32) Wang, J.; Li, L.; Morin, C.; Hitchcock, A. P.; Doran, A.; Scholl, A. J. *Electron Spectrosc.* **2009**, *170*, 25–36.
(33) Kikuma, J.; Tonner, B. P. *J. Electron Spectrosc. Relat. Phenom.* **1996**, *82*, 53–60.
(34) aXis2000 is free for non-commercial use. It is written in Interactive Data Language (IDL) and available from http://unicorn.mcmaster.ca/aXis2000.html
(35) Strang, G. *Linear Algebra and Its Applications*; Harcourt Bracourt, Jovanovich: San Diego, CA, 1988.
(36) Koprinarov, I. N.; Hitchcock, A. P.; McCrory, C. T.; Childs, R. F. *J. Phys. Chem. B* **2002**, *106*, 5358–5364.

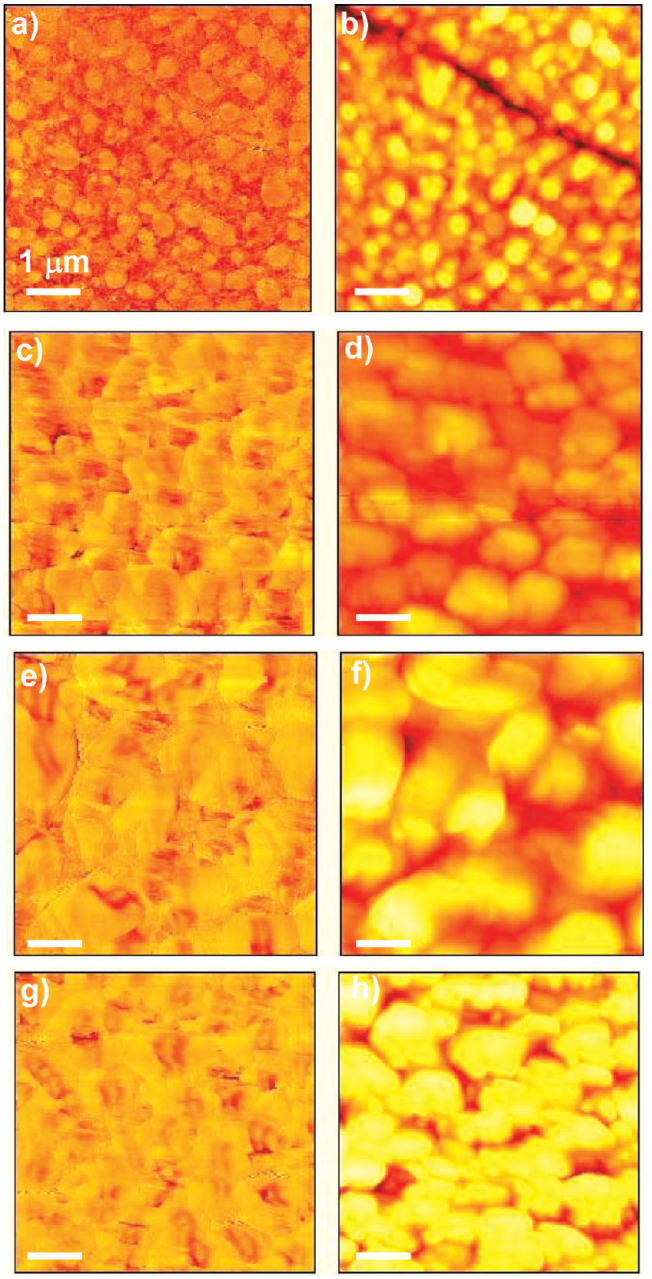

Figure 3. AFM phase mode images of PS:PEO thin film blends spun cast from a 1 wt % dichloromethane solution loaded with (a) 20:80 w/w ratio, (c) 40:60 ratio, (e) 60:40 ratio, and (g) 80:20 ratio. AFM height mode images: (b) 20:80 ratio, (d) 40:60 ratio, (f) 60:40 ratio, and (h) 80:20 ratio. AFM images are 5 μm $\times$ 5 μm.

a threshold mask was applied to each component map to isolate specific pixels corresponding to PS, PEO, or the interface. Figure 2b shows the color coded combination of the masks used in this example. The averaged spectrum from all pixels with a component signal above a threshold value was extracted. The resulting average NEXAFS spectrum for each of the three regions was further modified by setting the pre-edge intensity to zero. The spectra of each region (Figure 2c,d,e) were then fit to the pre-edge background subtracted PS, PEO and HSA reference spectra. Several stacks obtained from different regions of the same sample were analyzed as independent repeat measurements and the final quantitative results were averaged with the uncertainties from these multiple determinations used as the standard deviation.

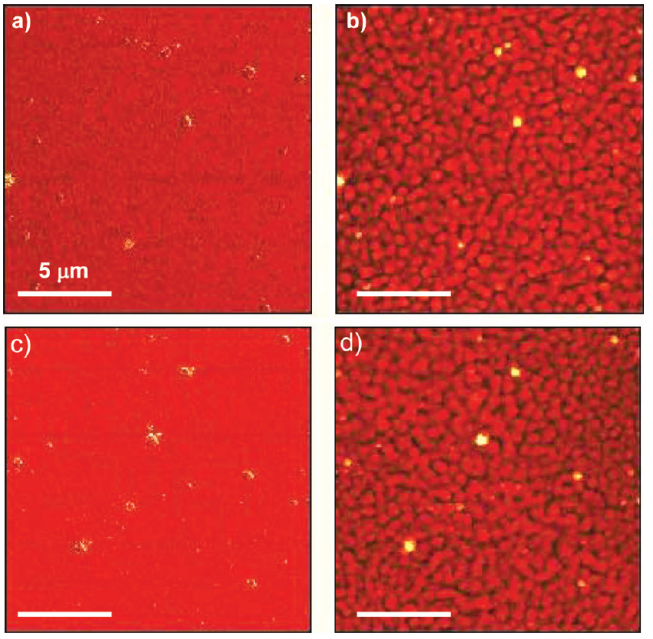

Figure 4. AFM phase mode images of PS:PEO thin film blends spun cast from a 0.5 wt % dichloromethane solution loaded with (a) 40:60 w/w ratio and (c) 60:40 ratio. AFM height mode images: (b) 40:60 ratio and (d) 60:40 ratio. AFM images are 15 μm $\times$ 15 μm.

3. Results and Discussion

3.1. Substrate Characterization. *3.1.1. Atomic Force Microscopy (AFM).* Four films with PS:PEO 20:80, 40:60, 60:40 and 80:20 w/w composition were spun cast from dichloromethane (1 wt %), UV cross-linked, and imaged with AFM. These films are ~300 nm thick as determined by AFM imaging across a scratch in each film (results not shown). AFM *phase* mode images (Figure 3a,c,e,g) reveal interesting microstructure in the 500− 2000 nm range for all four films. The similar color shading in all four phase images indicates that similar phases/polymer components exist at each surface. The *height* mode images (Figure 3b,d,f,h) show that the more yellow-colored domains increase in size laterally from ~500 to 1000 nm, as the PS:PEO ratio changes from 20:80 to 80:20. Naively these domain size changes would suggest that the small domains seen in the PS:PEO 20:80 film and the larger domains seen in the PS:PEO 80:20 film are composed mainly of PS. However, polymer identity is difficult to determine by AFM without polymer destruction or verification with a chemically sensitive technique,[37−39] and there are many cases known where there is little or no correlation between bulk and surface composition.[42]

Samples for X-PEEM analysis need to be considerably thinner in order to have adequate conductivity to avoid charging that occurs along extruded structures (ie. low rugosity films are required). Thus, in order to obtain samples suitable for X-PEEM analysis the PS:PEO 40:60 and 60:40 solutions were diluted to 0.5 wt % and spun cast under otherwise identical conditions. The height mode images shown in Figure 4 reveal a regular, randomly patterned film surface. A close inspection of the morphology of these films reveal that both the PS:PEO 40:60 and 60:40 surfaces are composed of a classic dispersed droplet morphology. The pattern from the height mode images is observed faintly in the

(37) Wang, P.; Koberstein, J. T. *Macromolecules* **2004**, *37*, 5671–5681.
(38) Walheim, S.; Ramstein, M.; Steiner, U. *Langmuir* **1999**, *15*, 4828–4836.
(39) Virgilio, N.; Favis, B. D.; Pepin, M.-F.; Desjardins, P.; L'Esperance, G. *Macromolecules* **2005**, *38*, 2368–2375.

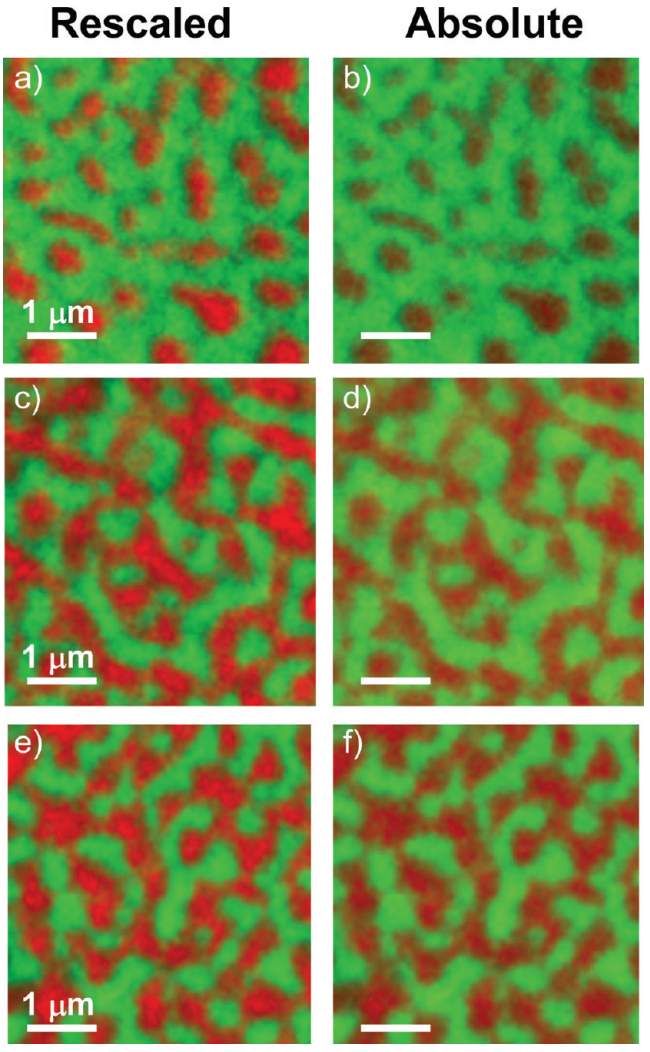

Figure 5. Color coded composite maps derived from C 1s X-PEEM image sequences of (a, b) 40:60 (w/w) PS:PEO, (c, d) 60:40 PS:PEO, and (e, f) 60:40 PS:PEO annealed films cast from 0.5 wt % dichloromethane solutions. The left-hand maps (a, c, e) are rescaled while the right-hand maps (b, d, f) are on an absolute scale. PS is coded red; PEO is coded green.

phase mode images, suggesting incomplete phase separation but to a relatively small extent since there is very minor color shading variation. The thicknesses of the PS:PEO 40:60 and 60:40 films determined by AFM across a scratch are 130(5) and 147(5) nm, respectively, suitable for X-PEEM analysis.

3.1.2. X-PEEM Analysis. Figure 5 presents two different presentations of the color coded composites of the PS and PEO component maps derived from SVD fitting of C 1s image sequences measured from the unannealed PS:PEO 40:60 and PS:PEO 60:40 thin films (0.5 wt % from CH_2Cl_2, UV irradiated to cross-link the PEO component). The rescaled maps are shown on the left, which presents the images with each component scaled separately to the full range (0−255) of its color, allowing for greater sensitivity to the spatial distribution of each component. The maps on the right are displayed on a common absolute scale (0−10 nm), which preserves the true compositional information.

The rescaled color coded images verify the different surface morphologies for the two films obtained from AFM, with the discrete domains of the PS and PEO exhibiting classical dispersed droplet and worm-like structures, respectively, for the PS:PEO 40:60 (Figure 5a) and 60:40 films (Figure 5c). As the mass ratio changes from PS:PEO 40:60 to 60:40, a phase inversion is seen as the red-colored PS component alters from discrete domains to the continuous phase, and vice versa for the green-colored PEO component. For polymers with similar viscosities, the phase inversion point occurs when the composition of two blended polymers is approximately equal,[40] which in this case is close to 50:50. The cross-linked PEO regions are bright green in the absolute images of the PS:PEO 40:60 (Figure 5b) and 60:40 films (Figure 5d), suggesting these regions are pure PEO. In contrast, the red PS regions for both films show a much more green color indicative of incomplete phase segregation.

Table 1. Composition of PS and PEO (nm/pixel) in the PS-Rich and PEO-Rich Regions of PS:PEO Blends with Respect to Polymer Ratios, Total Polymer Concentration and Annealing (Uncertainty ±0.5 nm[a])

		polymer ratios PS:PEO		annealing
region	component	40:60	60:40	PS:PEO 60:40 18 h at 160 C
PS	PS	4.4	7.1	7.4
	PEO	5.6	2.9	2.6
PEO	PS	1.8	3.3	3.4
	PEO	8.2	6.7	6.6

[a] Uncertainty estimated from repeat measurements over several different areas.

The X-PEEM spectral fitting results obtained for the two polymer thin films quantifies the partial phase separation (Table 1). Here, the PS or PEO region is defined as the pixels with the most red or green color, respectively, and is considered especially "PS-rich" or "PEO-rich". For the PS:PEO 40:60 substrate, the quantitative analysis indicates that the PEO region is dominated by 8.2(5) nm of PEO while only 1.8(5) nm of PS is detected. This small amount of PS likely arises from trapped PS microdomains with sizes below the spatial resolution of the X-PEEM microscope. The dominant component in the PS region for this film is also PEO (5.5(5) nm) with only 4.4(5) nm of detected PS.

Similar quantitative results are observed for the PEO-rich region of the PS:PEO 60:40 film. The PEO-rich region is dominated by 6.7(5) nm of PEO signal, with 3.3(5) nm of detected PS. In contrast, the PS-rich region of this film reveals a greater thickness of PS (7.1(5) nm), resulting from the higher concentration of PS in this system. Still, 2.9(5) nm of PEO is detected, showing that this film remains only partially phase segregated.

Since solvent-cast blends are thermodynamically unequilibrated due to rapid solvent evaporation, the thin film substrates may reach equilibrium by annealing above the glass transition temperature (T_g), leading to greater phase separation.[41] After vacuum annealing for 18 h at 160 °C, above the T_g of both polymers (PS T_g, 110 °C;[42] PEO T_g, −60 °C[43]), the quantitative analysis obtained from X-PEEM (Supporting Information, Figure 2) revealed no difference between the annealed and unannealed films (uncertainty ±0.5 nm). Even with annealing, some PEO is still seen in the PS region (Table 1) which we interpret as a surface enrichment of the PEO. While it is true the X-PEEM signal is an integration over the outermost 10 nm, it is also most sensitive to the outer few nm.

(40) Miles, I. S.; Zurek, A. *Polymer* **1988**, *28*, 796–805.
(41) Ton-That, C.; Shard, A. G.; Daley, R.; Bradley, R. H. *Macromolecules* **2000**, *33*, 8453–8459.
(42) Morin, C.; Ikeura-Sekiguchi, H.; Tyliszczak, T.; Cornelius, R.; Brash, J. L.; Hitchcock, A. P.; Scholl, A.; Nolting, F.; Appel, G.; Winesett, D. A.; Kaznacheyev, K.; Ade, H. J. *Electron Spec.* **2001**, *121*, 203–224.
(43) Rashkov, I.; Manolova, N.; Li, S. M.; Espartero, J. L.; Vert, M. *Macromolecules* **1996**, *29*, 50–56.

In theory, the surface free energy of each polymer component is useful for predicting surface enrichment, with the lower surface free energy polymer segregating toward the air.[44] In this case, PS has a lower surface free energy (γ_{PEO} = 44 mJ/m^2 and γ_{PS} = 41.0 mJ/m^2 [45,46]). X-ray photoemission spectroscopy (XPS) of blends of low molecular weight diblock and triblock copolymers of PS/PEO and PEO/PS/PEO in various solvents showed PS surface enrichment in the top 5 nm of the film surface.[47,48] However, low molecular weight polymers (10−30 K) were used, followed by several applications of dip-coating, which is a more equilibrated method of creating thin films compared to spin coating.[46] Moreover, the characterization of these surfaces was carried out only with nonspatially resolved XPS. Spatially resolved X-PEEM analysis has the ability to detect surface enrichment of PEO even in the PS region.

Furthermore, polar PEO is likely more soluble in polar dichloromethane relative to PS, such that PEO stays dissolved longer in solution and upon spin coating develops an overlayer on the surface.[49] Surface enrichment of PEO has also been found with chitosan blends of PEO[50] and copolymers of PEO-*g*-PMMA (γ_{PMMA} = 40.2 mJ/m^2) and was attributed to the bulk composition and low T_g of PEO.[45] Since the T_g of PEO is low, PEO segments have greater flexibility and movement compared to PS, and thus more PEO is proposed to move toward the surface compared to PS.[45]

Although the PS:PEO 60:40 film exhibits incomplete phase segregation, protein adsorption to this surface is expected to provide insight into (1) evaluating protein adsorption to the PEO cross-linked, discrete domains, (2) examining how protein adsorption to a PS surface changes with incorporation of PEO, and (3) comparison of the PS:PEO system to the PS:PLA surface previously characterized by X-PEEM.[24]

3.2. Protein Adsorption. *3.2.1. Protein Adsorption to the PS−PEO Surface*. The unannealed PS:PEO 60:40 film was exposed to 0.005, 0.01, and 0.05 mg/mL HSA, followed by examination with X-PEEM. The rescaled images reveal significant color changes compared to the pure PS−PEO substrate, indicative of protein adsorption to the surface (Figure 6a,c,e). At all three concentrations, the blue color representing protein is most concentrated at the interface between PS and cross-linked PEO. This is the area of the lowest free energy.[42] As the concentration of HSA increases, the PS region changes from red to pink, suggesting a greater amount of blue HSA adsorbing to the surface while the color of the green PEO discrete domains remains similar, suggesting cross-linked PEO is more protein resistant compared to PS.

The absolute images for the 0.005 and 0.01 mg/mL HSA samples show red and green images comparable to the native substrate, signifying a low amount of adsorbed protein (Figure 6b,d). At the highest concentration of 0.05 mg/mL HSA, the red color of the PS continuous phase is darker, suggesting a small adsorbed contribution from the protein. The green color of the discrete domains remains sharply bright, revealing little adsorbed HSA (Figure 6f).

The quantitative results indicate that for all concentrations examined, HSA shows preferential adsorption to the interface between the PS and cross-linked PEO domains, which is the area of the lowest free energy (Table 2). As the concentration of HSA increases, the thickness of the protein detected on the PS region is almost doubled from 0.005 mg/mL to 0.05 mg/mL. In contrast, the thickness of detected protein on the cross-linked PEO domains is the same within uncertainties, suggesting that cross-linked PEO is protein resistant at the highest concentration examined (0.05 mg/mL HSA). Still, cross-linked PEO is not completely protein resistant since 0.7−1.0 nm of HSA is detectible on the domains.

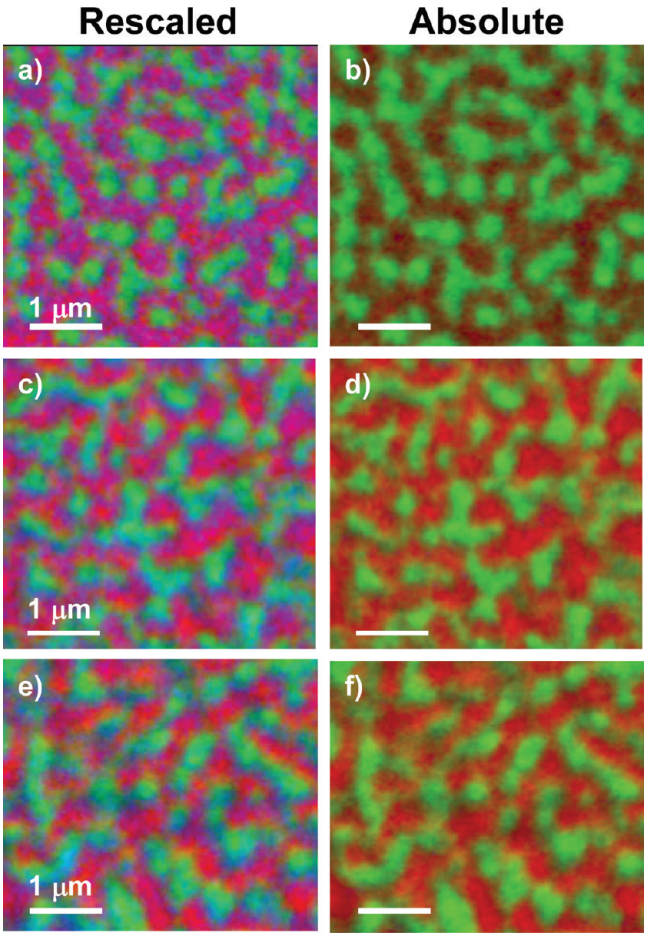

Figure 6. Color coded composite maps derived from C 1s X-PEEM image sequences of (a, b) 0.05 mg/mL HSA, (c, d) 0.01 mg/mL HSA, and (e, f) 0.005 mg/mL HSA adsorbed to an unannealed 60:40 PS:PEO film, 0.5 wt % loading. The left-hand maps (a, c, e) are rescaled while the right-hand maps (b, d, f) are on an absolute scale. PS is coded red, PEO is coded green, and HSA is coded blue.

Table 2. Thickness (nm) of PS, PEO, and HSA in the PS, PEO, and Interface Regions from PS:PEO 60:40 (0.5 wt %) Films Exposed to 0.05, 0.01, and 0.005 mg/mL HSA from DDI Water (Uncertainty: ±0.5 nm)

region	composite thickness (nm)	HSA concentration (mg/mL) 0.05	0.01	0.005
PS	PS	6.1	6.5	6.9
	PEO	3.1	2.7	2.6
	HSA	0.8	0.8	0.5
PEO	PS	2.7	3.8	3.1
	PEO	7.1	5.2	6.2
	HSA	0.8	1.0	0.7
interface	PS	4.8	4.7	4.9
	PEO	4.3	4.0	4.2
	HSA	1.0	1.3	1.0

(44) Davies, M. C.; Shakesheff, K. M.; Shard, A. G.; Domb, A.; Roberts, C. J.; Tendler, S. J. B.; Williams, P. M. *Macromolecules* **1996**, *29*, 2205–2212.
(45) Guo, S.; Shen, L.; Feng, L. *Polymer* **2001**, *42*, 1017–1022.
(46) Ton-That, C.; Shard, A. G.; Teare, D. O. H.; Bradley, R. H. *Polymer* **2001**, *42*, 1121–1129.
(47) Thomas, H. R.; O'Malley, J. J. *Macromolecules* **1979**, *12*, 323–329.
(48) O'Malley, J. J.; Thomas, H. R.; Lee, G. M. *Macromolecules* **1979**, *12*, 996–1001.
(49) Ton-That, C.; Shard, A. G.; Daley, R.; Bradley, R. H. *Macromolecules* **2000**, *33*, 8453–8459.
(50) Amiji, M. M. *Biomaterials* **1995**, *16*, 593–599.

Previously, we characterized PEO films with the addition of 1.5%, 5%, and 10% PETA and found that below a PETA concentration of 1.5% no adsorbed HSA was detectable via X-PEEM.[51] The amount of PETA used for these PS−PEO cross-linked films is 1%. Thus, PETA should not significantly contribute to the detected 0.7−1.0 nm of HSA adsorbed on the cross-linked PEO domains. Instead, the adsorption of HSA probably arises from the incomplete phase segregation of the PS−PEO films, since the PEO-rich area shows 33% contribution from PS.

Furthermore, a PS:PEO 60:40 film (0.5 wt %) with no PETA and no UV cross-linking was exposed to a 0.005 mg/mL HSA solution (Supporting Information, Figure 3) for 20 min. The color coded micrographs show very red absolute images, indicative of PS as the dominant component within the top 10 nm of the film surface. Although most of the PEO dissolved in solution, some PEO-rich areas were found. Likely, in these regions the PEO polymer chains were entwined with PS and anchored to the surface.

The quantitative results verify that PS dominates (60−80%) the entire surface (Supporting Information, Table 1) with only 3.6 nm of PEO detected in the PEO-rich region. More importantly, the amount of HSA detected on the surface of the noncross-linked PS−PEO film is within the uncertainty of the amount of HSA detected on the cross-linked PS−PEO film, verifying that at the low PETA concentration used, the cross-linker does not affect HSA adsorption to the PEO-rich regions in this study.

Recently, lectin adsorption to a phase segregated blend of PS−PEO was examined with fluorescence microscopy via integral geometry analysis.[52] These authors found that lectin adsorbed selectively to the PS regions with no detectable binding to the PS−PEO interface. From X-PEEM, our results clearly show that the interface is composed of almost 50:50 PS:PEO, and thus the hydrophobic contribution from PS likely results in the increased adsorption of HSA to our interface.

3.2.2. Comparison to a PS−PLA Spun Cast Surface. In comparison to the PS−PLA 40:60 (0.7 wt %) spun-cast substrate previously characterized by X-PEEM,[24] at low concentrations of HSA (0.005 and 0.01 mg/mL HSA) similar protein thicknesses are detected on the PS continuous domains. At higher concentrations (0.05 mg/mL HSA) a significant decrease (0.8 nm) in protein thickness is detected on the PS regions of the PS−PEO blend compared to the PS−PLA blend. This increased protein resistance is attributed to the incomplete phase segregation of PS and PEO in the PS region for the pure substrate. Since the PS area is composed of ∼70% PS and ∼30% PEO, a significant fraction of high molecular weight PEO is incorporated in this region. This allows for the possibility of extended loops of PEO along the PS surface, which may contribute to the increased protein repellency.

The suppression of protein adsorption, platelet adhesion, and activation, by PEO has also been observed for monomethyl ether-PEG-*b*-PLA blends,[53] polysulfone- (PSf-) *g*-PEO,[4] and blends of chitosan and PEO[50] via XPS and electron spectroscopy for chemical analysis. In the case of the PSf-*g*-PEO film with 56% grafted low molecular weight PEO (MW 750), no adsorbed bovine serum albumin (BSA) was detected by XPS.[4] We speculate that using densely grafted PS-*g*-PEO may provide even greater protein resistance compared to the high MW PEO used in this study. While X-PEEM is an excellent technique for simultaneously probing both the protein and substrate, one limitation is that the exact chemical interface where the HSA molecule adsorbs is not fully defined due to the integration over the ∼10 nm sampling depth.

Studies using multiple proteins or plasma solutions will also be of interest. Previous, Grainger et al[54] reported that although the minimum amount of protein adsorption for single protein solutions were found on the surfaces with 40% PEO ratios, the same protein repellency was not found for plasma solutions, suggesting that single protein experiments may be too much of a simplification relative to the *in vivo* processes.

4. Conclusions

PS−PEO films spun cast from dichloromethane with various mass ratios and concentrations were characterized by AFM and X-PEEM. Our results show incomplete phase segregation of PS and PEO. The surface enrichment of PEO in the PS region leads to enhanced protein repellency upon protein adsorption. PEO is cross-linked with a very low concentration of PETA and it was found that 1% PETA does not affect protein adsorption to the PEO. Rather, incomplete phase segregation of the film with 33% PS in the PEO-rich regions led to the detection of 0.7−1.0 nm HSA adsorbed to the PEO discrete domains.

Acknowledgment. This research is supported by the Natural Science and Engineering Research Council (NSERC, Canada), AFMNet and the Canada Research Chair programs. X-ray microscopy was carried out using PEEM2 and STXM532 at the ALS. The ALS is supported by the US Department of Energy under Contract DE-AC03-76SF00098.

Supporting Information Available: Figures showing AFM images and colro-coded component maps and a table of thickness and concentration data for the polymers. This material is available free of charge via the Internet at http://pubs.acs.org.

(51) Leung, B. O.; Hitchcock, A. P.; Brash, J. L.; Scholl, A.; Doran, A. *Adv. Biomater.: Adv. Eng. Mater*. **2010**, *12*, B133–B138.
(52) Zemla, J.; Lekka, M.; Raczkowska, J.; Bernasik, A.; Rysz, J.; Budkowski, A. *Biomacromolecules* **2009**, *10*, 2101–2109.
(53) Lucke, A.; Tessmar, J.; Schnell, E.; Schmeer, G.; Gopferich, A. *Biomaterials* **2000**, *21*, 2361–2370.
(54) Grainger, D. W.; Okano, T.; Kim, S. W. *J. Colloid Interface Sci*. **1989**, *132*, 161–175.